IEEE Access
Multidisciplinary | Rapid Review | Open Access Journal

Received August 29, 2020, accepted September 14, 2020, date of publication September 21, 2020,
date of current version September 29, 2020.

Digital Object Identifier 10.1109/ACCESS.2020.3025330

Sensing Characteristics of Fiber Fabry-Perot Sensors Based on Polymer Materials

ZHENG-DA LIU[1], BIN LIU[1], JUAN LIU[1], YANJUN FU[1], MENGYU WANG[1], SHENG-PENG WAN[1], XINGDAO HE[1], JINHUI YUAN[2], (Senior Member, IEEE), HAU-PING CHAN[3], (Member, IEEE), AND QIANG WU[1,4]

[1]Key Laboratory of Nondestructive Test (Ministry of Education), Nanchang Hangkong University, Nanchang 330063, China
[2]Research Center for Convergence Networks and Ubiquitous Services, University of Science and Technology Beijing, Beijing 100083, China
[3]Department of Electrical Engineering, City University of Hong Kong, Hong Kong
[4]Faculty of Engineering and Environment, Northumbria University, Newcastle Upon Tyne NE1 8ST, U.K.

Corresponding authors: Bin Liu (liubin_d@126.com), Jinhui Yuan (yuanjinhui81@163.com), and Qiang Wu (qiang.wu@northumbria.ac.uk)

This work was supported in part by the Natural Science Foundation of Jiangxi under Grant 20192ACBL21051, Grant 20192ACB20031, and Grant 20172BCB22012; and in part by the National Natural Science Foundations of China under Grant 61665007, Grant 11864025, and Grant 61665007.

ABSTRACT A simple optic-fiber Fabry-Perot (FP) sensing technique was proposed and experimentally investigated by using polymer material to connect the ends of two singlemode fibers. Four different polymer materials (benzocyclobutene (BCB), UV88 (Relentless, China), Loctite3525 (HenKel, Germany), and NOA68 (Norland, USA)) filling the FP cavity were used to comparatively study the sensing performance of temperature, strain and refractive index. The result shows that the FP sensor with BCB has excellent repeatability with good linear response to temperature in a wide range from room temperature to 250 °C, which is much larger than that of other three materials (<90 °C), while UV88 with a cost of less than 1/10 of the other three polymer materials has the best sensitivity to strain and temperature. In addition, the FP sensor was firstly applied to measure ultraviolet (UV) light intensity. The test results demonstrate that the proposed FP sensor structure has a good linear response and repeatability to UV intensity for all four polymer materials, and Loctite3525 has the highest sensitivity (0.0087 nm/(mw/cm^2)) and the best repeatability among the four polymer materials.

INDEX TERMS Optical fiber sensor, Fabry-Perot cavity, polymer materials, ultraviolet sensing.

I. INTRODUCTION

An optical fiber Fabry-Perot (FP) sensor is a type of interference sensor [1], which can be used for sensing of temperature [2]–[6], strain [7]–[10], refractive index (RI) [11]–[13], pressure [14]–[16], magnetic field [17], [18], sound pressure [19] and so on. It has been studied widely in the past decades and applied in wide areas such as aerospace, petrochemical, energy, civil and other special industries due to its advantages of small size, lightweight, fast response. immunity to electromagnetic field and remote operation [20], [21].

There are different methods to fabricate optical fiber FP sensors [22]. For example, the dual-beam FP interferometer has a relatively low cost, and better stability under severe conditions [23], and thus is the most common FP sensor structure. In 2012, Liao *et al* manufactured a FP RI sensor using high powerlaser etching and welding technique [24], which isn't cost effective. In 2016, Liu used a fusion splice to connect a chemically-etched multimode fiber and a singlemode fiber (SMF) to fabricated a high-sensitivity FP strain sensor [25]. In the same year, Xu *et al* fabricated a high-pressure FP measurement sensor by connecting a short section hollow core fiber with an SMF, where a silicon dioxide diaphragm was coated at the end of HCF section to form an FP cavity [26]. However, the sensitivity is relatively low due to the low thermo-optic effect of silica fiber. A FP interferometer using (ultraviolet) UV polymer droplets was prepared in 2015 by Sun *et al.* [27]. In 2018, Oliveira *et al* used UV glue to fill the FP cavity to make FP sensor [28], and Zhao *et al* used polyimide film as FP cavity for humidity sensing [29]. The use of polymer materials makes the fabrication process simple with additional advantage of low cost and high sensitivity to temperature and strain due to the high thermo-optic and elastic effect of polymer materials.

The associate editor coordinating the review of this manuscript and approving it for publication was Sukhdev Roy.

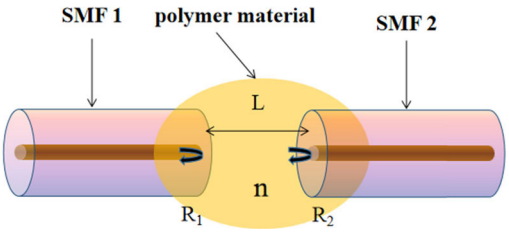

FIGURE 1. A schematic diagram of the optics-fiber FP structure.

In the case of UV sensing, narrow band gap semiconductors Si and GaAs are widely used to sense UV intensity. However, their UV sensitivity is relatively low [30], and the semiconductor material is normally sensitive to infrared and visible light and thus cause cross-effects [31]–[33]. Moreover, the processing semiconductor material is usually complicated and the cost is high.

In this paper, a simple FP cavity manufacturing technique is proposed by using polymer material to fill the gap between the ends of two SMFs. The sensing responses of four different polymer materials (UV88, NOA68, Loctite3525 and BCB) for strain, temperature and RI were tested and analyzed. Furthermore, a new application for UV sensing with the FP sensor was proposed, and experimental results showed that it has a good sensitivity and linear response to UV intensity without cross-sensitivity to visible light.

II. THEORETICAL ANALYSIS

The schematic diagram of the proposed optical fiber FP sensor is shown in Fig. 1. There are two reflection interfaces in the FP structure: one is at the interface between SMF 1 and filled polymer material (R_1) and the other is at the interface between the polymer material and SMF 2 (R_2). Assume the reflectivity $R_1 = R_2 = R$ and the RI of the F-P cavity (polymer material) is n, the reflected light intensity I_R is [22]:

$$I_R = \frac{2R[1 - \cos(4\pi nL/\lambda)]}{1 + R^2 - 2R\cos(4\pi nL/\lambda)} I_0 \quad (1)$$

where L, λ and I_0 are cavity length, wavelength and input light intensity, respectively. When R is relatively low ($R \leq 5\%$), the reflected light intensity I_R can be expressed:

$$I_R = 2R[1 - \cos(4\pi nL/\lambda)] \quad (2)$$

III. FABRICATION OF THE FIBER FP STRUCTURES

A section SMF (YOFC, China) was prepared for fabrication of the sensor. Four different polymer materials, UV88 (Relentless, China), Loctite3525 (HenKel, Germany), NOA68 (Norland, USA) and BCB (an optical waveguide resin material) were used to fill in the gap of the optical fiber FP cavity, to investigate the influence of these polymer materials on the performance of the FP sensor. UV88, Loctite3525 and NOA68 are composed of oligomer, active diluent, photosensitizer and auxiliary agent, and the ratio of various components is also different. BCB is composed of photosensitizer and BCB monomer. The physical properties of the four polymer materials are listed in Table 1.

TABLE 1. Properties values of four polymer materials.

Polymer material	Properties				
	Refractive index	Viscosity (cps)	Hardness (Shore)	Young's modulus [mpa)]	Elongation (%)
UV88	-	7500	DA70	-	160
NOA68	1.54	5000	DA60	135	80
Loctite3525	1.51	15000	DA68	25	160
BCB	1.541	870	-	2000	6

The manufacturing set-up of optic-fiber FP structure which consists of two continuous zoom telecentric lens and a three-dimensional translation stage, is shown in Fig. 2(a). UV curing light source (SPCM-0800, China), thermostat (Sunne, China) and electric iron (China) were used to cure the polymer materials. The fabrication process is divided into five steps as illustrated in Fig. 3(a):

i. Cut two SMFs with flat end surface by using a traditional fiber cleaver (CT30, Japan), and rough one end of the output SMF to reduce background reflection with a sandpaper.
ii. Fix one SMF onto a metal block and another SMF onto a 3-D translation stage, which can precisely align the two SMFs.
iii. FP cavity lengths can be controlled by adjusting the translation stage along the axial direction of the fiber.
iv. Use a drop of polymer material to fill gap between two SMFs, which is effectively the FP cavity of the fiber sensor.
v. Cure the polymers with different conditions: UV88, Locatite3525 and NOA68 are cured for 20 seconds by UV light source, followed 12 h curing at 70 °C; BCB were cured 20 seconds by UV light source firstly, and then heated at 300 °C for 10 seconds.

Figures 2(b) and (c) show the microscope photos of fabricated optical fiber FP structures filled with NOA68 and BCB, respectively.

Figure 3(b) shows a schematic diagram of the experimental setup, which consists of a broadband source (MAX-RAY PHOTONICS, China), an optical spectrum analyzer (OSA, YOKOGAWA AQ5370D, Japan) and a circulator. The reflective spectra of the FP sensors of four different polymer materials with cavity length of 40 μm (Polymer material will shrink after curing, which will also cause the deviation of the cavity length) were shown in Figs. 4(a)-(d).

IV. EXPERIMENTS AND ANALYSIS

Firstly, the strain responses of the FP sensors filled with above four polymer materials were tested and compared. The schematic diagram of the experimental setup for strain sensing is shown in Fig. 5. The sensor is fixed on a translation

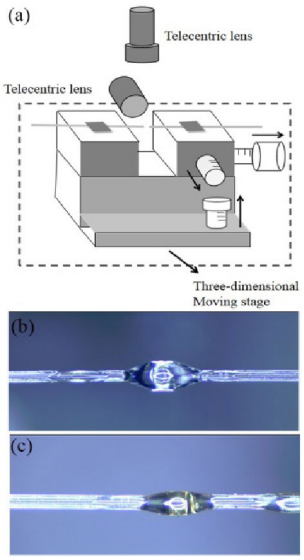

FIGURE 2. (a) Sensor fabrication set-up; (b) Sensor made of NOA68; (c) Sensor made of BCB.

stage and the axial strain f can be expressed as:

$$f = \frac{\Delta L}{L_0}, \tag{3}$$

In the experiments, the distance between the two fixed points is $L_0 = 2$ cm and the step change of the strain applied to the sensor is 50 $\mu\varepsilon$.

Figures 6(a), (b) and (c) show the spectral responses vs. increasing and decreasing strain applied to the sensors filled with UV88, NOA68 and BCB. The spectra of the three materials was red-shifted because the cavity length of the sensor was changed after applying strain to the fiber FP sensor, the material RI also changes due to the stress-light effect. As a result, the spectrum experienced a drift. The strain sensitivity is related to Young's modulus and viscosity of the material. The sensor strain $f(t)$ can be expressed as [34]:

$$f(t) = f_0\left[1 + \exp(\frac{-E}{v}t)\right], \tag{4}$$

where f_0 is a time-independent stress component, E, v and t are Young's modulus, viscosity and time. Arnaldo G. Leal-Junior *et al.* concluded that the stress applied to the material has a negative effect on Young's modulus and a positive effect on the viscosity [34]. This conclusion has been verified in our experiments. The positive and reverse travel strain sensing curves in Figs 6(d), (e) and (f) demonstrated good linearity between strain and wavelength shift for these three materials. BCB has the largest Young's modulus and the smallest viscosity, so it has the lowest sensitivity of 0.0032 nm/$\mu\varepsilon$. NOA68 has the second-largest Young's modulus and the second-smallest viscosity, so it has a greater sensitivity of 0.1198 nm/ $\mu\varepsilon$. The sensitivity value of UV88 is 0.2021 nm/ $\mu\varepsilon$. By contrast, FP sensor with UV88 is more sensitive to strain changes than that of NOA68 and BCB, due to its smallest Young's modulus and largest viscosity. It is worth noting that strain sensitivity is not linearly related to Young's modulus and viscosity. The data of Loctite3525 is missing in Figs. 6, because the spectrum for Loctite3525 showed a red-shift when a stress was put on the sensor. When the translation stage rotates 1 μm, which spectrum suddenly changes greatly and continuously red shifts. However, this sensor could not be obtained for stress sensing characteristics due to an unstable spectrum. We think it may be caused by its high sensitivity because its Young's modulus is very small and its viscosity is very large.

In addition, the hysteresis error is used to measure the hysteresis phenomenon, that the positive and reverse travel

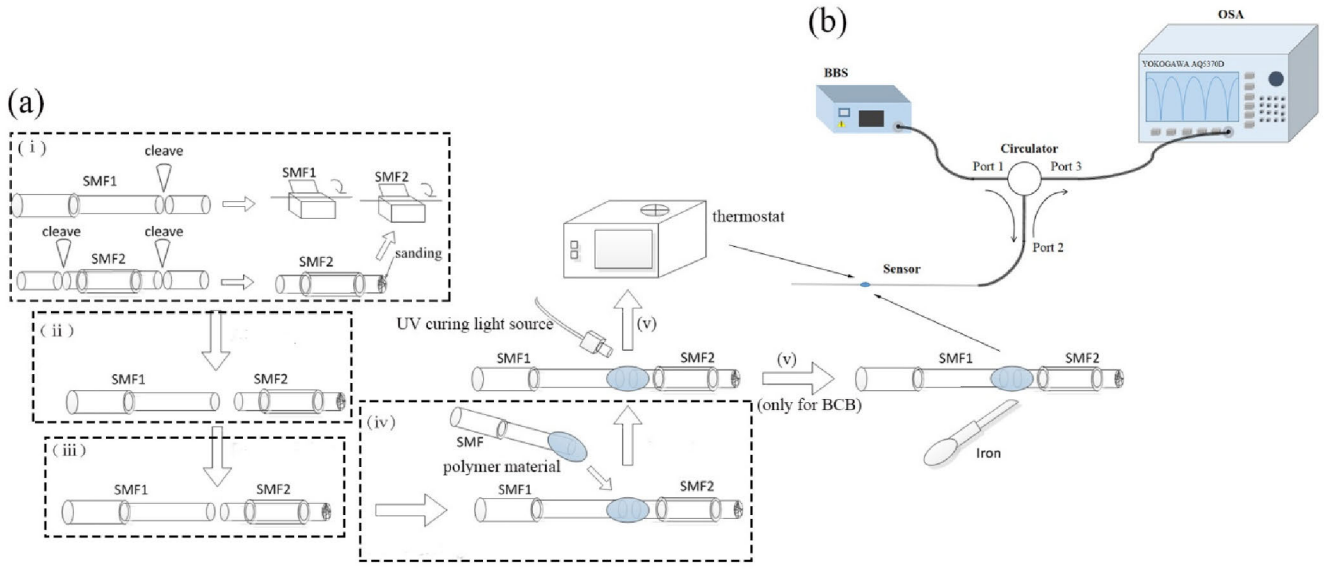

FIGURE 3. (a) The production process of sensor, (b) The experimental device.

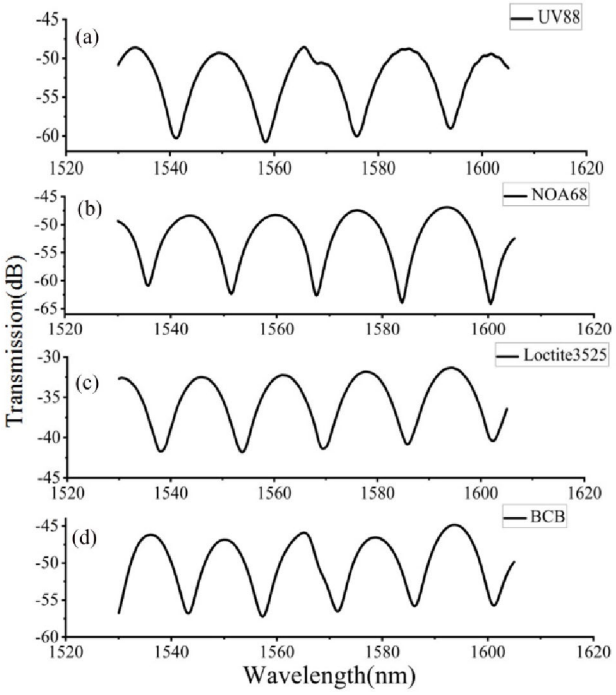

FIGURE 4. Reflection spectra of the FP structures of different polymer materials with FP cavity length $L = 40$ μm: (a) UV88, (b) NOA68, (c) Loctite3525 and (d) BCB.

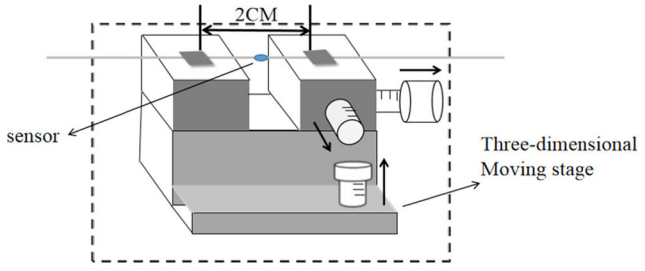

FIGURE 5. A schematic diagram of the strain measurement setup.

sensing curves do not coincide, can described as:

$$H = \frac{\Delta_{\max}}{y_{\max}}, \tag{5}$$

where Δ_{max} and y_{max} are the maximum hysteresis difference in the full range and the output full range. The hysteresis errors of strain sensing are calculated as 0.1102, 0.024 and 0.003 nm/$\mu\varepsilon$ for UV88, NOA68 and BCB, respectively.

Next, temperature responses of the FP sensors filled with the above four polymer materials were studied. In our experiments, the sensor was heated gradually in a temperature control box, and the spectral responses were recorded by an OSA (Data is recorded every 5 °C for UV88, NOA68 and Loctite3525 and every 10 °C for BCB). The spectral responses of the above four FP sensors vs. increasing and decreasing temperature are shown in Figs. 7(a), (b), (c) and (d), respectively. As temperature increase, the wavelength shifts to longer wavelength for all the above four sensors. The reason is that the temperature variation changes the RI

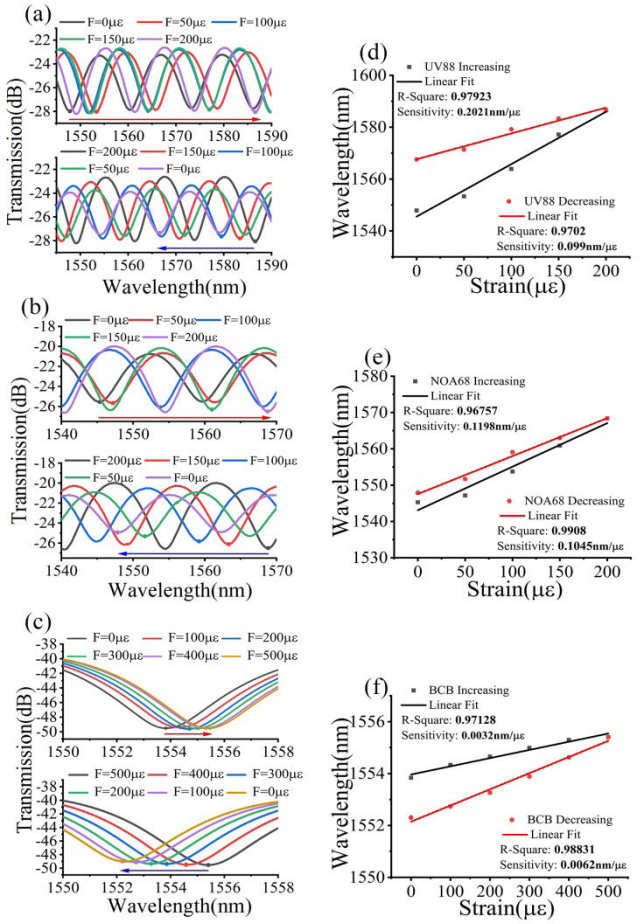

FIGURE 6. Reflection spectra response versus stress for the fiber FP structure with (a) UV88, (b) NOA68 and (c) BCB; (d)-(f) Dip wavelength shift as a function of stress.

and dimension of the polymer material, which can be described as:

$$\left(\frac{\Delta n}{n} + \frac{\Delta L}{L}\right) = (\alpha + \xi)\,\Delta T, \tag{6}$$

where α and ξ are thermal expansion effect coefficient and thermo-optical effect coefficient, respectively. The maximum temperature measured by the FP sensors filled with UV88, Nor68 and Loctite3525 is about 90 °C. When the temperature is higher than 90 °C, those polymers will be soften and thus not suitable for temperature measurement higher than 90 °C.

For BCB, the highest measurable temperature can reach as high as 250 °C. The positive and reverse travel temperature sensing curves in Figs 7(e)-(h) demonstrated a good linearity between temperature and dip wavelength shift for the FP sensor filled with above four different polymer materials. The temperature rising sensitivities of UV88, Nor68, Loctite3525 and BCB are 1.3355, 0.968, 0.938 and 0.2164 nm/°C, respectively. UV88 has the highest temperature sensitivity. and the temperature cooling sensitivities of UV88, Nor68, Loctite3525 and BCB are 1.3085, 1.3597, 1.044 and 0.2185 nm /°C, respectively. It cannot be ignored that the sensitivity of heating and cooling is not the same, where the worst repeatability material is NOA68.

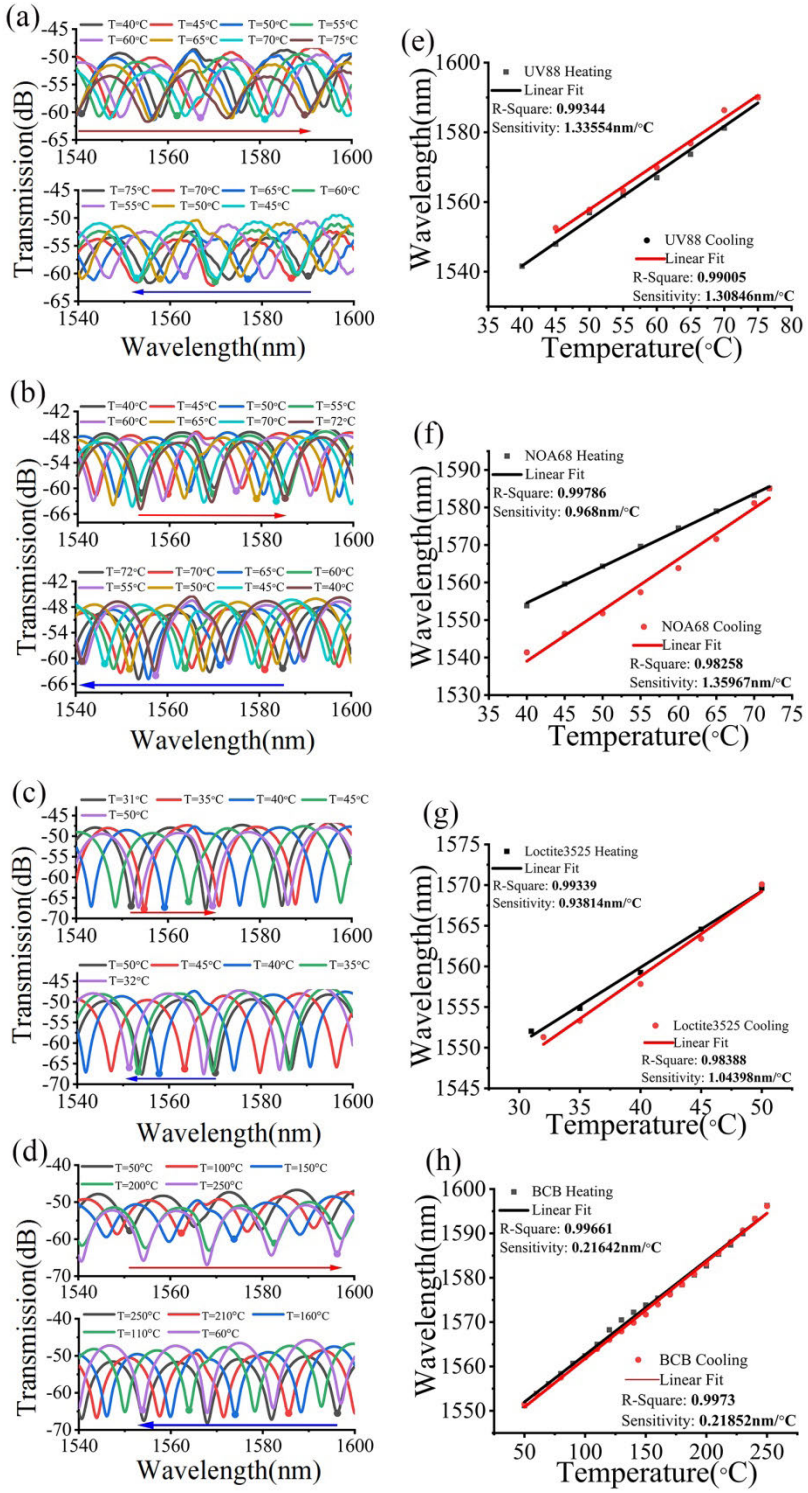

FIGURE 7. Reflection spectra response versus temperature for the fiber FP structure with (a) UV88, (b) NOA68, (c) Loctite3525 and (d) BCB; (e)-(h) Dip wavelength shift as a function of temperature.

The hysteresis errors of temperature sensing are 0.1536, 0.3885, 0.0599 and 0.0112 nm/°C for UV88, NOA68, Loctite3525 and BCB, respectively. It may be that the temperature has changed the properties of the material. For BCB, although the temperature sensitivity is lower than the above three polymer materials, it can measure temperatures up to 250 °C and has good repeatability and hysteresis. In addition, the price of UV88 is far less than of the other three materials, which shows a high-cost performance. Therefore, according to the requirements of different temperature measurement

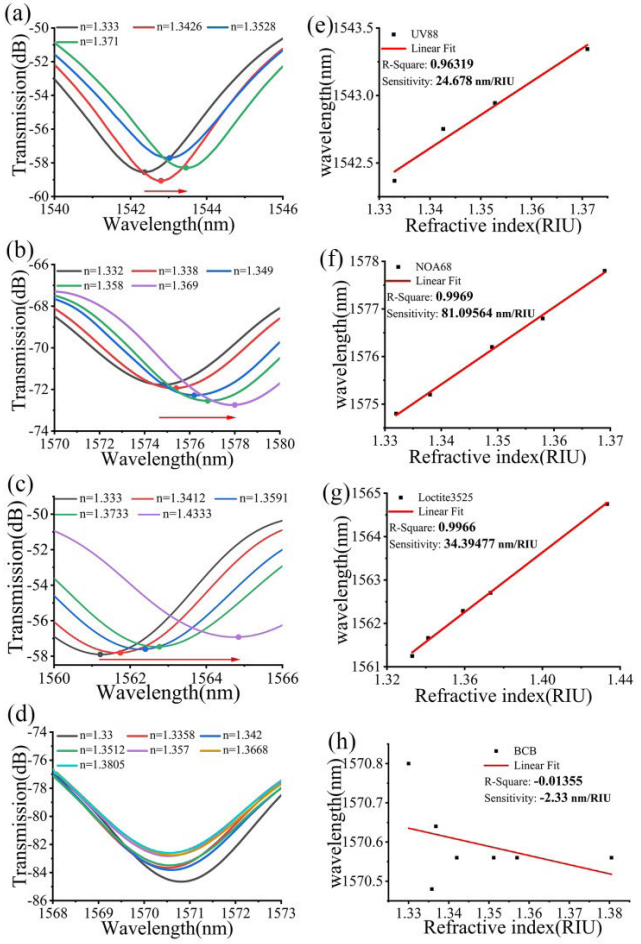

FIGURE 8. Reflection spectra response versus RI for the fiber FP structure with (a) UV88, (b) NOA68, (c) Loctite3525 and (d) BCB; (e)-(h) Dip wavelength shift as a function of RI.

range and sensitivity, different polymer materials can be selected to prepare optic-fiber FP temperature sensor.

Although the polymer materials have been cured, but the waterproof performance is not very good. Therefore, the refractive index solution infiltrates into the polymer FP cavity, resulting in the response of the FP sensor to surrounding RI. We put the sensor in pure water completely, after waiting for the spectrum to stabilize, using a dropper to drop Dimethyl sulfoxide(It can increase the refractive index of the solution), recording the spectrum when it becomes stable, and repeating the operation several times to obtain multiple sets of spectra. The RI responses of the FP structure filled with these polymer materials are tested in experiment. Figs. 8(a), (b) and (c) demonstrated that the spectra with UV88, Nor68 and Loctite3525 have red-shift as increasing of surrounding RI. It is possible the polymer material hasn't completely filled the space between the fibers. The optical path difference increases as RI, which can be described as:

$$OPD = 2nL, \tag{7}$$

where n, L are the refractive index and length of the FP cavity. The corresponding RI sensitivities of UV88, Nor68 and Loctite3525 are 24.678, 81.096 and 34.394 nm/RIU, respectively

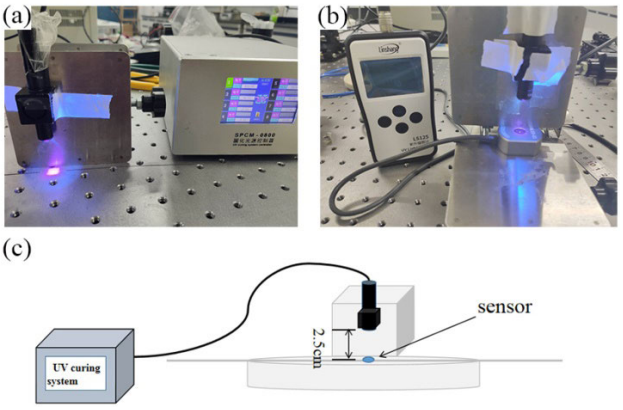

FIGURE 9. (a) UV sensing device; (b) Calibration of UV intensity; (c) Device schematic.

[shown in Figs. 8(e), (f) and (g)]. But for BCB which waterproof performance is excellent, we found that the reflection spectrum has no significant shift with increasing of surrounding RI [shown in Figs. 8(d) and (h)], the FP structure with BCB has residual sensitivity to RI, which can be used to avoid the problem of cross-sensitivity between temperature and refractive index in temperature sensing applications.

The proposed FP sensor is applied for UV sensing. Figure 9(a) shows an experimental photo for UV light intensity sensing. An UV radiometer (linshang-125, China) is used for calibration of UV light intensity [shown in Fig. 9(b)] and Fig. 9(c) shows a schematic diagram of the UV sensing setup. Figures 10(a), (b), (c) and (d) show the spectral responses and repeatability to UV intensity for the FP sensor filled with UV88, NOA68, Loctite3525 and BCB, respectively. The results show that, for all the four sensors, the wavelength undergoes red-shift and blue-shift as UV intensity increases and decreases respectively. The reason is the fact that increase of UV intensity will introduce the increase of RI of the polymer materials, resulting in the red-shift of the FP sensor. Good linear fits for their sensors were demonstrated in Figs. 10(e), (f), (g) and (h), and the sensitivities are calculated as 0.0067, 0.00573, 0.00834 and 0.0023 nm/(mw/cm^2), respectively. Moreover, the good hysteresis for UV sensing was demonstrated by calculating the hysteresis errors [8.56×10^{-4}, 2.37×10^{-4}, 3.8×10^{-4} and 2.39×10^{-4} nm/(mw/cm^2) for UV88, NOA68, Loctite3525 and BCB]. FP sensor filled with Loctite3525 has both highest sensitivity than that of other three materials. Therefore, it has become the first choice for UV intensity measurement. The resolution of UV light measured by the spectrometer could reach 0.733 mw/cm^2, and it also was found to be insensitive to visible light, showing low cross sensitivity to visible light and thus is an idea sensor for UV intensity measurement.

Finally, through the integration and comparison of the above experimental results, the temperature, stress, RI and UV light intensity sensing characteristics of the optics-fiber FP structures filled with UV88, Loctite3525, NOA68 and BCB are completely summarized in Table 2.

TABLE 2. Sensing Summarized sensing characteristics values of the proposed sensor.

Material	Sensitivity						
	Strain (nm/με)		Temperature (nm/°C)		RI (nm/RIU)	UV light intensity [nm/(mw/cm^2)]	
	Increasing	Decreasing	Heating	Cooling		Increasing	Decreasing
UV88	0.2021	0.099	1.3355	1.3085	24.678	0.0067	0.0058
NOA68	0.1198	0.1045	0.968	1.3597	81.096	0.00573	0.00532
Loctite3525	-	-	0.938	1.044	34.395	0.00834	0.0078
BCB	0.0032	0.0062	0.2164	0.2185	Insensitive	0.0023	0.00225

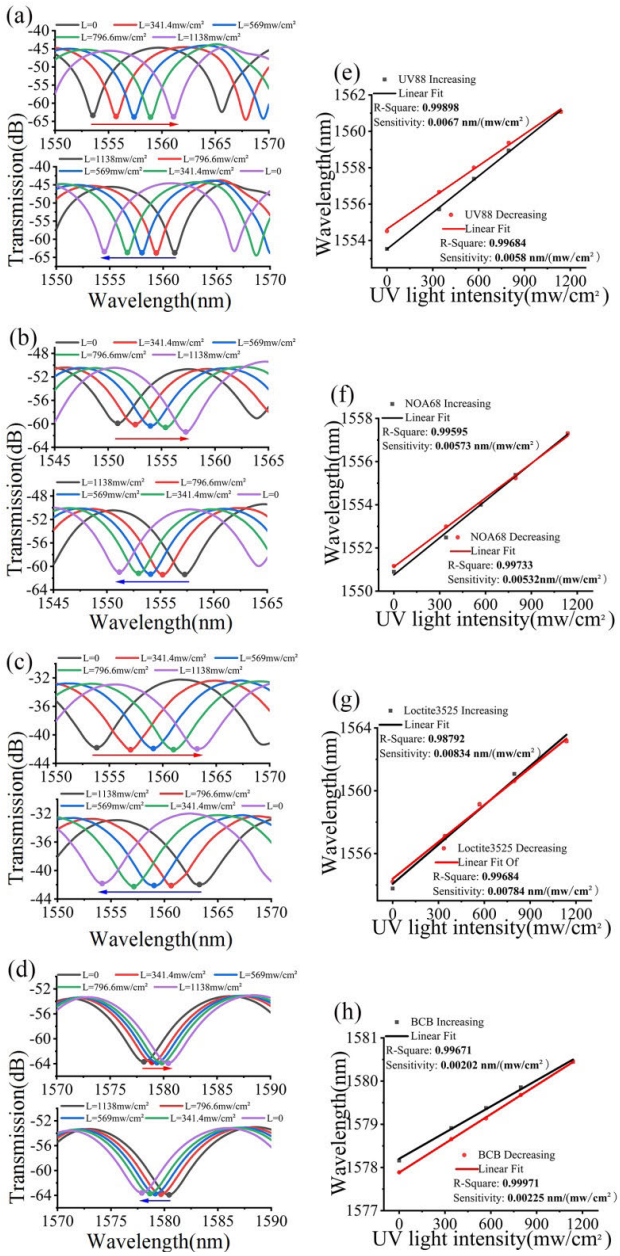

FIGURE 10. Reflection spectra response versus UV light intensity for the fiber FP structure with (a) UV88, (b)NOA68, (c) Loctite3525 and (d)BCB; (e)-(h) Dip wavelength shift as a function of UV light intensity.

V. CONCLUSION

A simple and low-cost optical fiber FP sensor structure was proposed by filling polymer materials (UV88, Locatite3525, NOA68 and BCB) between the ends of two SMFs. The sensing performance to strain, temperature, RI and UV light intensity were studied experimentally for the four different polymer materials. The results show that UV88 has the best sensitivity to both strain and temperature with sensitivity of 0.2021 nm/$\mu\varepsilon$ and 1.3355 nm/°C, respectively. The FP sensor filled with BCB has wide temperature measurement range from room temperature to 250 °C, although its temperature sensitivity is as low as 0.2164 nm/°C. In addition, the FP sensors filled with the four polymer materials can measure the change of UV light intensity, where the sensor filled with Loctite3525 has the highest sensitivity of 0.0087 nm/(mw/cm^2) to UV intensity compared to that of the other three polymer materials. The proposed sensors can be used in aerospace, electric power, astronomical observation technologies, fire alarm, missile launch and other scenarios that require temperature, strain or UV measurement [35], [36].

REFERENCES

[1] T. Yoshino, K. Kurosawa, K. Itoh, and T. Ose, "Fiber-optic Fabry–Pérot interferometer and its sensor applications," *IEEE Trans. Microw. Theory Techn.*, vol. 30, no. 10, pp. 1612–1621, Oct. 1982.

[2] C. Zhu, Y. Y. Zhuang, B. H. Zhang, M. Roman, P. P. Wang, and J. Huang, "A miniaturized optical fiber tip high-temperature sensor based on concave-shaped Fabry–Pérot cavity," *IEEE Photon. Technol. Lett.*, vol. 31, no. 1, pp. 35–38, Jan. 1, 2019.

[3] H. Gao, Y. Jiang, Y. Cui, L. C. Zhang, J. S. Jia, and J. Hu, "Dual-cavity Fabry–Pérot interferometric sensors for the simultaneous measurement of high temperature and high pressure," *IEEE Sensors J.*, vol. 18, no. 24, pp. 10028–10033, Dec. 2018.

[4] T. Wei, Y. Han, H. L. Tsai, and H. Xiao, "Miniaturized fiber inline Fabry–Pérot interferometer fabricated with a femtosecond laser," *Opt. Lett.*, vol. 33, no. 6, pp. 536–538, 2008.

[5] S. Pevec and D. Donlagic, "Miniature all-fiber Fabry–Pérot sensor for simultaneous measurement of pressure and temperature," *Appl. Opt.*, vol. 51, no. 19, pp. 4536–4541, 2012.

[6] G. Zhang, M. Yang, and M. Wang, "Large temperature sensitivity of fiber-optic extrinsic Fabry–Pérot interferometer based on polymer-filled glass capillary," *Opt. Fiber Technol.*, vol. 19, no. 6, pp. 618–622, 2013.

[7] T. Zhao, Y. Gong, J. Y. Rao, Y. Wu, Z. L. Ran, and H. J. Wu, "Fiber-optic Fabry–Pérot strain sensor based on graded-index multimode fiber," *Chin. Opt. Lett.*, vol. 9, no. 5, 2011, Art. no. 050602.

[8] Y. Zhao, M.-Q. Chen, R.-Q. Lv, and F. Xia, "In-fiber rectangular air Fabry–Pérot strain sensor based on high-precision fiber cutting platform," *Opt. Commun.*, vol. 384, pp. 107–110, Feb. 2017.

[9] J. Zhang, G. D. Peng, L. Yuan, and W. M. Sun, "Composite-cavity-based Fabry–Pérot interferometric strain sensors," *Opt. Lett.*, vol. 32, no. 13, pp. 1833–1835, 2007.

[10] G. K. B. Costa, P. M. P. Gouvêa, L. M. B. Soares, J. M. B. Pereira, F. Favero, A. M. B. Braga, P. Palffy-Muhoray, A. C. Bruno, and I. C. S. Carvalho, "In-fiber Fabry–Pérot interferometer for strain and magnetic field sensing," *Opt. Express*, vol. 24, no. 13, p. 14690, 2016.

[11] M. Deng, T. Zhu, Y.-J. Rao, and H. Li, "Miniaturized fiber-optic Fabry–Pérot interferometer for highly sensitive refractive index measurement," in *Proc. 1st Asia–Pacific Opt. Fiber Sensors Conf.*, Chengdu, China, Aug. 2008, pp. 1–4.

[12] G. Yuan, G. Yu, Y. J. Rao, Z. Tian, W. Yu, and Z. L. Ran, "Sensitivity analysis of hybrid fiber Fabry–Pérot refractive-index sensor," *Acta Phys. Sinica*, vol. 60, no. 6, 2011, Art. no. 064202.
[13] F. Xu, L. Lu, W. Lu, and B. L. Yu, "In-line Fabry–Pérot refractive index sensor based on microcavity," *Chin. Opt. Lett.*, vol. 11, no. 8, pp. 93–96, 2013.
[14] J. Ma, J. Ju, L. Jin, and W. Jin, "A compact fiber-tip micro-cavity sensor for high-pressure measurement," *IEEE Photon. Technol. Lett.*, vol. 23, no. 21, pp. 1561–1563, 2011.
[15] C. Liao, S. Liu, L. Xu, C. Wang, Y. Wang, Z. Li, Q. Wang, and D. N. Wang, "Sub-micron silica diaphragm-based fiber-tip Fabry–Pérot interferometer for pressure measurement," *Opt. Lett.*, vol. 39, no. 10, p. 2827, 2014.
[16] Y. Wang, D. N. Wang, C. Wang, and T. Hu, "Compressible fiber optic micro-Fabry–Pérot cavity with ultra-high pressure sensitivity," *Opt. Express*, vol. 21, no. 12, p. 14084, 2013.
[17] P. Zhang, M. Tang, F. Gao, B. Zhu, S. Fu, J. Ouyang, P. P. Shum, and D. Liu, "Fabry–Pérot interferometric sensor based on metglas ribbon and hollow-core photonic crystal fiber for magnetic field measurement," in *Proc. FBTA*, Wuhan, China, 2014, Paper FF4B.4.
[18] R.-Q. Lv, Y. Zhao, D. Wang, and Q. Wang, "Magnetic fluid-filled optical fiber Fabry–Pérot sensor for magnetic field measurement," *IEEE Photon. Technol. Lett.*, vol. 26, no. 3, pp. 217–219, Feb. 1, 2014.
[19] Y. Zhao, M.-Q. Chen, F. Xia, and R.-Q. Lv, "Small in-fiber Fabry–Pérot low-frequency acoustic pressure sensor with PDMS diaphragm embedded in hollow-core fiber," *Sens. Actuators A, Phys.*, vol. 270, pp. 162–169, Feb. 2018.
[20] V. Bhatia and A. M. Vengsarkar, "Optical fiber long-period grating sensors," *Opt. Lett.*, vol. 21, no. 9, pp. 692–694, 1996.
[21] T. Zhu, D. Wu, M. Liu, and D.-W. Duan, "In-line fiber optic interferometric sensors in single-mode fibers," *Sensors*, vol. 12, no. 8, pp. 10430–10449, Aug. 2012.
[22] W. M. Chen, X. H. Lei, W. Zhang, X. M. Liu, and C. R. Liao, "Recent progress of optical fiber Fabry–Pérot sensors," *Acta Phys. Sinica*, vol. 38, no. 3, 2018, Art. no. 0328010.
[23] C. Ma and A. Wang, "Signal processing of white-light interferometric low-finesse fiber-optic Fabry–Pérot sensors," *Appl. Opt.*, vol. 52, no. 2, p. 127, 2013.
[24] C. R. Liao, T. Y. Hu, and D. N. Wang, "Optical fiber Fabry–Pérot interferometer cavity fabricated by femtosecond laser micromachining and fusion splicing for refractive index sensing," *Opt. Express*, vol. 20, no. 20, p. 22813, 2012.
[25] Y. Liu, D. N. Wang, and W. P. Chen, "Crescent shaped Fabry–Pérot fiber cavity for ultra-sensitive strain measurement," *Sci. Rep.*, vol. 6, no. 1, Dec. 2016, Art. no. 38390.
[26] J. S. Xu, J. He, W. Huang, X. Z. Xu, K. K. Guo, Z. Zhang, and Y. P. Wang, "Suppression of parasitic interference in a fiber-tip Fabry–Pérot interferometer for high pressure measurements," *Opt. Express*, vol. 26, no. 22, pp. 28178–28185, 2018.
[27] B. Sun, Y. Wang, J. Qu, C. Liao, G. Yin, J. He, J. Zhou, J. Tang, S. Liu, Z. Li, and Y. Liu, "Simultaneous measurement of pressure and temperature by employing Fabry–Pérot interferometer based on pendant polymer droplet," *Opt. Express*, vol. 23, no. 3, p. 1906, 2015.
[28] R. Oliverra, L. Bilro, and R. Nogueira, "Fabry–Pérot cavities based on photopolymerizable resins for sensing applications," *Opt. Mater. Express*, vol. 8, no. 8, pp. 2208–2221, 2018.
[29] Y. Zhao, Y. Yuan, W. Gan, and M. Yang, "Optical fiber Fabry–Pérot humidity sensor based on polyimide membrane: Sensitivity and adsorption kinetics," *Sens. Actuators A, Phys.*, vol. 281, pp. 48–54, Oct. 2018.
[30] J.-L. Zhang, Y.-X. Nan, H.-G. Li, W.-M. Qiu, X. Yang, G. Wu, H.-Z. Chen, and M. Wang, "A new wide bandgap organic semiconductor and its application in organic UV sensors with tunable response wavelength," *Sens. Actuators B, Chem.*, vol. 162, no. 1, pp. 321–326, Feb. 2012.
[31] F. Hossein-Babaei, M. M. Lajvardi, and F. A. Boroumand, "Large area Ag–TiO_2 UV radiation sensor fabricated on a thermally oxidized titanium chip," *Sens. Actuators A, Phys.*, vol. 173, no. 1, pp. 116–121, Jan. 2012.
[32] H.-G. Li, G. Wu, H.-Z. Chen, and M. Wang, "Polymer/ZnO hybrid materials for near-UV sensors with wavelength selective response," *Sens. Actuators B, Chem.*, vol. 160, no. 1, pp. 1136–1140, Dec. 2011.
[33] N. A. M. Asibab, F. S. Husairiab, K. A. Eswarad, A. N. Afaahab, M. H. Mamatc, M. Rusopac, and Z. Khusaimiab, "Developing high-sensitivity UV sensors based on ZnO nanorods growth on TiO_2 seed layer fifilms using solution immersion method," *Sens. Actuators A, Phys.*, vol. 302, p. 11827, Feb. 2019.
[34] A. G. Leal-Junior, C. R. Díaz, C. Marques, A. Frizera, and M. J. Pontes, "Analysis of viscoelastic properties influence on strain and temperature responses of Fabry–Pérot cavities based on UV-curable resins," *Opt. Laser Technol.*, vol. 120, Dec. 2019, Art. no. 105743.
[35] Y. Jin, J. Wang, B. Sun, J. C. Blakesley, and N. C. Greenham, "Solution-processed ultraviolet photodetectors based on colloidal ZnO nanoparticles," *Nano Lett.*, vol. 8, no. 6, pp. 1649–1653, Jun. 2008.
[36] Z. Yang, M. Wang, X. Song, G. Yan, Y. Ding, and J. Bai, "High-performance ZnO/Ag nanowire/ZnO composite film UV photodetectors with large area and low operating voltage," *J. Mater. Chem. C*, vol. 2, no. 21, pp. 4312–4319, 2014.

ZHENG-DA LIU is currently pursuing the degree with the School of Measuring and Optical Engineering, Nanchang Hangkong University. His research interest includes fiber optic sensing.

BIN LIU received the B.S. and Ph.D. degrees from Sun Yat-sen University, China. He is currently an Associate Professor with the Key Laboratory of Nondestructive Test (Ministry of Education), Nanchang Hangkong University, China. His main research interest includes fiber optic sensing.

JUAN LIU received the Ph.D. degree from Beijing Normal University, China. She is currently a Lecturer with the Key Laboratory of Nondestructive Test (Ministry of Education), Nanchang Hangkong University, China. Her main research interest includes fiber optic sensing.

YANJUN FU received the Ph.D. degree from the Huazhong University of Science and Technology of China. He is currently a Professor with the Key Laboratory of Nondestructive Test (Ministry of Education), Nanchang Hangkong University, China. His main research interests include photoelectric detection technology, photoelectric imaging, and 3D measurement.

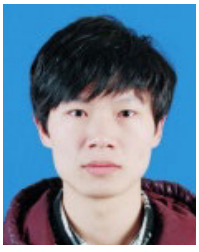

MENGYU WANG received the bachelor's degree from the Harbin Institute of Technology, in 2015. He is currently pursuing the Ph.D. degree in instrument science and technology with the University of Science and Technology of China. He joined the Key Laboratory of Nondestructive Test (Ministry of Education), Nanchang Hangkong University, China, in 2019. His research interests include optical resonator, fiber optics, crystal optics, optical sensors, and laser spectrum.

SHENG-PENG WAN received the B.S. and Ph.D. degrees from the University of Electronic and Technology of China. He is currently a Professor with the Key Laboratory of Nondestructive Test (Ministry of Education), Nanchang Hangkong University, China. His main research interest includes fiber optic sensing.

XINGDAO HE was born in Jingan, China, in 1963. He received the Ph.D. degree in optics from Beijing Normal University, Beijing, China, in 2005. He is currently a Professor with the Key Laboratory of Nondestructive Test (Ministry of Education), Nanchang Hangkong University, China. His current research interests include light scattering spectroscopy, optical holography, and information processing.

JINHUI YUAN (Senior Member, IEEE) received the Ph.D. degree in physical electronics from the Beijing University of Posts and Telecommunications (BUPT), Beijing, China, in 2011. He is currently a Professor with the Department of Computer and Communication Engineering, University of Science and Technology Beijing (USTB). He was selected as a Hong Kong Scholar with the Photonics Research Centre, Department of Electronic and Information Engineering, The Hong Kong Polytechnic University, in 2013. He has published over 200 papers in the academic journals and conferences. His current research interests include photonic crystal fibers, silicon waveguide, and optical fiber devices. He is a Senior Member of OSA.

HAU-PING CHAN (Member, IEEE) received the Ph.D. degree in integrated optics with the Electronic Department, The Chinese University of Hong Kong, in 1991. He joined the Department of Electrical Engineering, City University of Hong Kong, where he is currently an Associate Professor. He has over 25 years of research experiences in the design, fabrication, and characterization of integrated optical devices for communication and sensing applications, waveguides materials and processing, photonic and electronic packaging, reliability and failure analysis, and fabrication of polymer optical fiber for THz application. He has published over 200 papers in international journals and conferences and co-owns three patents. He is a member of OSA.

QIANG WU received the B.S. degree from Beijing Normal University, in 1996, and the Ph.D. degree from the Beijing University of Posts and Telecommunications, Beijing, China, in 2004. From 2004 to 2006, he worked as a Senior Research Associate with the City University of Hong Kong. From 2006 to 2008, he was a Research Associate with Heriot-Watt University, Edinburgh, U.K. From 2008 to 2014, he worked as a Stokes Lecturer with the Photonics Research Centre, Dublin Institute of Technology, Ireland. He is currently an Associate Professor/Reader with the Faculty of Engineering and Environment, Northumbria University, Newcastle Upon Tyne, U.K. He has over 200 publications in the area of photonics and holds three invention patents. His research interests include optical fiber interferometers for novel fiber optical couplers and sensors, nanofiber, microsphere sensors for bio-chemical sensing, the design and fabrication of fiber Bragg grating devices and their applications for sensing, nonlinear fibre optics, surface plasmon resonant, and surface acoustic wave sensors. He is an Editorial Board Member of Scientific Reports, an Associate Editor of the IEEE Sensors Journal, and an Academic Editor of the*Journal of Sensors*.